Density-functional studies of excited states of silicon nanoclusters

Olli Lehtonen and Dage Sundholm
Department of Chemistry, P. O. Box 55 (A. I. Virtasen Aukio 1), FIN-00014 University of Helsinki, Helsinki, Finland
(Received 15 February 2005; revised manuscript received 19 April 2005; published 8 August 2005)

The molecular structures of $Si_{29}H_{24}$, $Si_{29}H_{36}$, and $Si_{35}H_{36}$ clusters in the ground state as well as in the lowest singlet and triplet excited states have been studied at the density-functional theory level using the first-order linear-response-theory approach for the singlet excited state. Structural changes compared to the ground state due to Franck-Condon relaxation of the singlet excited state are small, whereas optimization of the lowest triplet state is found to result in a dissociation of a Si—Si bond. The electronic excitation spectra up to 5 eV for the ground-state and excited-state structures of the silicon nanoclusters are also reported. The obtained Franck-Condon shift for the first excited state of $Si_{29}H_{36}$ is 0.70 eV, yielding a luminescence energy of 3.14 eV which is in good agreement with experimental data. The Franck-Condon shifts for $Si_{29}H_{24}$ and $Si_{35}H_{36}$ are found to be 1.17 and 1.67 eV, yielding emission energies of 1.57 and 2.03 eV, respectively, which are significantly smaller than the experimental value of about 3 eV. Thus, the present study supports the notion that the silicon nanoclusters fabricated through electrochemical etching consist of 29 Si atoms surrounded by 36 hydrogen atoms.

DOI: 10.1103/PhysRevB.72.085424 PACS number(s): 73.22.−f, 78.67.−n

I. INTRODUCTION

The discovery of the luminescent properties of porous silicon samples[1–3] initiated intense experimental and computational studies of silicon nanoparticles. Interesting research results involving nanosized silicon have been reported by, among others, Nayfeh and co-workers.[4–8] They fabricated nanosized silicon through electrochemical etching with hydrofluoric acid (HF). By using this technique they were able to disperse bulk Si into nanoparticles of about 1 nm in diameter. The obtained Si nanoparticles were found to be strongly luminescent exceeding the luminescence activity of fluorescein.[5,9] In addition to the strong distinct photoluminescence, they also found that the Si nanoparticles exhibit stimulated emission effects which is an important step toward the realization of a Si laser.[4,10] The Si nanoparticles were found to possess also other interesting optical properties such as directed light beam emission[7] and harmonic generation.[11] They are therefore showing promise for future silicon-based optical devices and applications. Although silicon nanoparticles have been the subject of many computational studies at *ab initio* and density-functional theory (DFT) levels of theory[7–9,11–18] the reason for their outstanding optical properties is still unresolved. Furthermore, a consensus concerning the molecular structure of the manufactured nanocrystals has not been reached either,[12,14,17,19] even though the size of the smallest ones is within the reach of accurate *ab initio* and DFT calculations.

The particle size has been determined by high-resolution transmission electron microscopy and confirmed by autocorrelation fluctuation spectroscopy.[8] By using computational *ab initio* and DFT approaches, a structural prototype consisting of 29 Si atoms was constructed.[9] This number of atoms was chosen since it is a magic number for clusters of T_d symmetry and with 29 Si atoms one obtains a cluster the size of which is about 1 nm.[8,9,20] The Si_{29} cluster of T_d symmetry has 36 dangling bonds, which at preparation react with the hydrogen in the bath of HF and H_2O_2, forming Si—H bonds on the cluster surface. For the Si cluster covered by 36 H atoms, Nayfeh *et al.* obtained a large band gap of 6 eV, indicating that $Si_{29}H_{36}$ is not the cluster they obtained in the etching process. They studied several cluster models computationally and came to the conclusion that $Si_{29}H_{24}$ is most likely the cluster they got in the test tube.[9,17]

However, DFT studies of the absorption and emission spectra[14,18] of the $Si_{29}H_{36}$ nanocluster yielded an optical gap in close agreement with the experimental excitation threshold of 3.7 eV. The corresponding coupled-cluster study of the absorption spectrum[14] employing a coupled-cluster singles and doubles model with the doubles contributions considered implicitly[21,22] (CC2) supported the obtained DFT results. The luminescence energy of 3.14 eV calculated at the DFT level also agreed well with the observed value.[18] Thus, these computational studies indicate that the Si atoms at the surface are connected to 36 hydrogens, yielding the $Si_{29}H_{36}$ cluster.

In this work, we extend the previous studies of Si nanocluster by calculating the electronic absorption and emission spectra for $Si_{29}H_{24}$, $Si_{29}H_{36}$, and $Si_{35}H_{36}$ which all are plausible candidates for the nanoparticles produced in the etching process. The Si cluster containing 35 Si atoms has previously been studied by Williamson *et al.*[23,24] and Friesner *et al.*,[15] and the optical gap of $Si_{29}H_{36}$ has also previously been calculated employing multireference second-order Møller-Plesset[25] and quantum Monte Carlo (QMC) methods.[26]

II. COMPUTATIONAL METHODS

The optimization of the molecular structure of the singlet ground states and of the first excited triplet states of the silicon nanoclusters were performed at the density-functional theory level using the gradient corrected Becke-Perdew (BP) functional,[27–29] which belongs to the functionals of the generalized gradient approximation (GGA) type. Triple-ζ

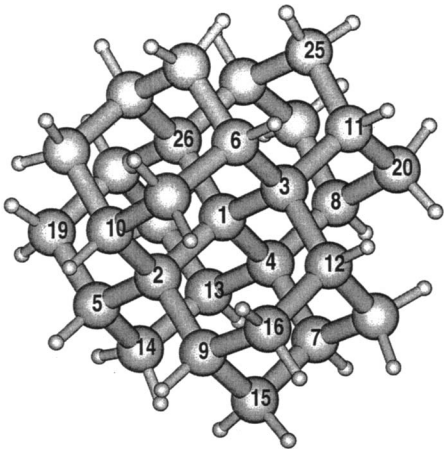

FIG. 1. The ground-state structure of $Si_{29}H_{36}$ and the numbering of the Si atoms. The structure of the first excited singlet state is visually almost identical.

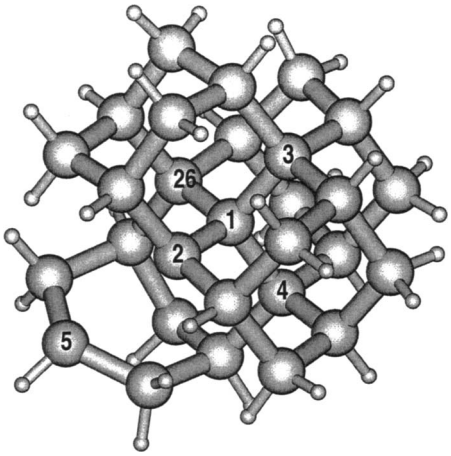

FIG. 2. The structure of the lowest triplet state of $Si_{29}H_{36}$ optimized at the BP DFT level using the TZVP basis sets.

valence-quality basis sets augmented with polarization functions[30] (TZVP) were used in most calculations. In the optimization of the triplet states, the unrestricted Kohn-Sham approach was employed. The electronic excitation spectra up to 5 eV were calculated using time-dependent density-functional theory (TDDFT).[31,32] The molecular structures of the first excited singlet and also of the lowest triplet states were optimized at the BP TDDFT level using analytical TDDFT gradients as implemented in the EGRAD module of TURBOMOLE.[33,34] For comparison, the molecular structures were also fully optimized using the Slater-Vosko-Wilk-Nusair (SVWN(v)) (Refs. 27, 35, and 36) local density approximation (LDA). The resolution of the identity (RI) approximation (also called density fitting) was employed in order to speed up the GGA and LDA computations.[37] The calculations on the silicon clusters were checked by employing the Perdew-Burke-Ernzerhof (PBE) functional,[38] the Tao-Perdew-Staroverov-Scuseria meta-GGA (TPSS) functional,[39] and Becke's three-parameter hybrid functional[40] with the Lee-Yang-Parr correlation functional[41] (B3LYP).

In the benchmark calculations on SiH_4, Si_2H_6, and Si_3H_8 the Karlsruhe quadruple-ζ valence basis sets augmented with double sets of polarization functions (QZVPP) were employed.[42] The TURBOMOLE program package[42] has been used in all calculations.

III. RESULTS

A. Structures

The optimization of the molecular structures of the ground state of the $Si_{29}H_{24}$, $Si_{29}H_{36}$, and $Si_{35}H_{36}$ clusters showed that their geometries belong to the T_d point group. The triply degenerate first excited singlet states (T_2) of $Si_{29}H_{24}$, $Si_{29}H_{36}$, and $Si_{35}H_{36}$ relax upon excitation yielding molecular structures belonging to the $C_s(A'')$, $D_{2d}(B_2)$, and $C_1(A)$ point groups, respectively. The symmetries of the first excited singlet states are given within parentheses. The molecular structures of $Si_{29}H_{36}$ in the singlet ground state and the fully relaxed structures of the ground and the first triplet excited states are shown in Figs. 1 and 2.

The structure optimization of the triplet state resulted in dissociation of one of the Si—Si bonds, as seen in Fig. 2. The Si—Si distance increased from 2.386 Å for the ground state to 4.322 Å in the first excited triplet state obtained using the unrestricted Kohn-Sham approach. The structure of the first triplet state was also optimized using the TDDFT

TABLE I. Comparison of calculated excitation wavelengths (in nm) for SiH_4, Si_2H_6, and Si_3H_8 with experimental data. Electronic transitions with oscillator strengths greater than 0.1 are reported. The excitation energies were calculated at the BP DFT and B3LYP DFT levels using QZVPP-quality basis sets. The molecular structures were optimized at the BP DFT level using the TZVP basis sets. The experimental wavelengths are taken from Ref. 44.

SiH_4			Si_2H_6			Si_3H_8		
BP	B3LYP	Expt.	BP	B3LYP	Expt.	BP[a]	B3LYP[b]	Expt.
138	134	141	171	165	164	201	195	187
129	125	128	155	141	147	176	180	165
113	111	116	148	136	131	167	168	133
			143	132	125	150	153	118
				131		148	145	

[a]Strong excitations were also obtained at 142, 138, 131, 130, 123, and 122 nm.
[b]Strong excitations were also obtained at 144, 142, 133, 131, 129, 124, and 123 nm.

method in combination with the BP functional. The BP TD-DFT structure optimization also resulted in a dissociation of the Si—Si bond. However, in this case, we were not able to obtain a fully converged molecular structure for the triplet state, since the spacings between the one-particle levels became very small due to the breaking of the Si—Si bond.

The BP DFT calculations clearly show that the molecular structure of the lowest triplet state involves long Si—Si bonds. The molecular structure of the triplet state of $Si_{29}H_{36}$ has previously been studied by employing plane waves and ultrasoft pseudopotentials. Franceschetti and Pantelides[13] obtained in their local spin-density calculation, a 15% (~0.35 Å) increase in one of the Si—Si bonds. In order to investigate this further, the molecular structures for the singlet ground state as well as for the first singlet and triplet excited states were fully optimized using the SVWN LDA functional. We did not obtain any significant differences between SVWN and BP structures of the singlet ground state and of the first singlet excited state. The structural differences are small with bond variations of less than 2 pm. The absorption and emission energies of 3.72 and 3.00 eV for $Si_{29}H_{36}$ obtained at the LDA level are also in close agreement with the ones calculated using the BP functional. However, the structure of the first triplet state optimized using the SVWN LDA functional turned out to be significantly different from that obtained with the BP functional. At the LDA level, no dissociation in any of the Si—Si bonds was observed, whereas optimization of the triplet state using the PBE GGA functional,[38] the TPSS meta-GGA functional, or the B3LYP hybrid functional[40,41] in combination with the TZVP basis sets led to dissociation of a Si—Si bond. The use of a split-valence basis set augmented with one set of polarization functions on the Si atoms in combination with the PBE functional resulted in a Si—Si bond elongation of only 0.280 Å (from 2.381 to 2.661 Å) showing that one has to use large basis sets and GGA functionals in order to obtain the correct molecular structure. At the LDA level using the TZVP basis sets, the largest bond elongation of 0.193 Å occurred for the Si—Si bond from the central Si to one of its nearest neighbors. It is well known that the LDA tends to overestimate bond strengths.[43] Thus, this is a further example where the LDA fails to give the correct molecular structure.

The molecular structure optimizations on the triplet states of the $Si_{29}H_{24}$ and $Si_{35}H_{36}$ clusters also yielded cluster structures with long dissociated Si—Si bonds. The bond dissociation occurs in one of the Si—Si bonds at the cluster surface. For $Si_{29}H_{24}$, the Si—Si bond length changes from 2.383 to 3.463 Å. The corresponding bond lengths for $Si_{35}H_{36}$ are 2.378 and 3.923 Å, respectively. These calculations show that the optimized triplet-state structure is not a good substitute for the optimized structure of the first excited singlet state, even though the dominating electron configuration of both the singlet and the triplet states can be obtained by the same single excitation from the ground state.

B. Absorption and emission spectra

1. General

A molecular system absorbing light is excited from the ground state in its equilibrium geometry to an excited state.

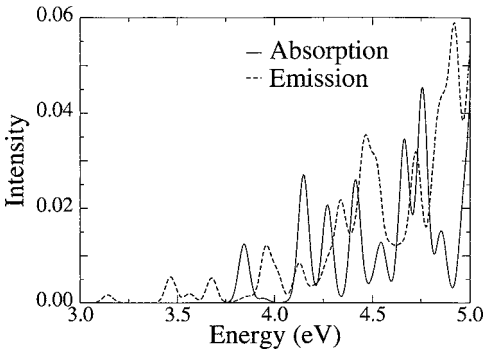

FIG. 3. The absorption and emission spectra of the $Si_{29}H_{36}$ cluster calculated at the BP DFT level using the TZVP basis sets.

In the excitation process the molecular structure is approximately unchanged; the excitation is usually thought to be vertical. Thus, the transition energies and band strengths of the absorption spectra should be calculated using the ground-state molecular structure.

The calculation of the emission spectra, the luminescence, is a much more involved task. The deexcitation giving rise to the luminescence is most likely close to vertical and the luminescence spectra should thus be calculated using the molecular structure of the excited state. The emission energy is redshifted compared to the absorption energy due to the structural relaxation of the excited state. Since the optimized molecular structure of the excited state is not completely optimal for the ground state, the ground-state energy for the excited-state structure is somewhat higher than for the ground-state geometry, also leading to a smaller emission energy, i.e., the mechanical strain introduced for the ground-state results is an additional contribution to the redshift of the excitation energy.

However, also other processes have to be considered in the simulation of luminescence spectra, since the intensity of the emitted light depends on the deexcitation route and the population of the levels. Both radiative and nonradiative transitions might play important roles. The final luminescence spectrum is a result of several competing coupled processes and can only be simulated by solving the rate equations for them. In this work, we have made no attempts to

TABLE II. The excitation energies (in eV) for the Si nanoclusters calculated using the ground-state (E_{abs}) and the first-excited-state (E_{emi}) structures. The Franck-Condon shift (ΔE_{FC}) and contributions from the ground-state (ΔE_{GS}) and excited-state (ΔE_{ES}) relaxations are also given.

	$Si_{29}H_{24}$	$Si_{29}H_{36}$	$Si_{35}H_{36}$
E_{abs}	2.74	3.84	3.70
E_{emi}	1.57	3.14	2.03
ΔE_{FC}	1.17	0.70	1.67
ΔE_{GS}	0.48	0.40	1.19
ΔE_{ES}	0.44	0.30	0.48
f_{abs}	0.000011	0.012	0.0027
f_{emi}	0.0000057	0.0017	0.00044

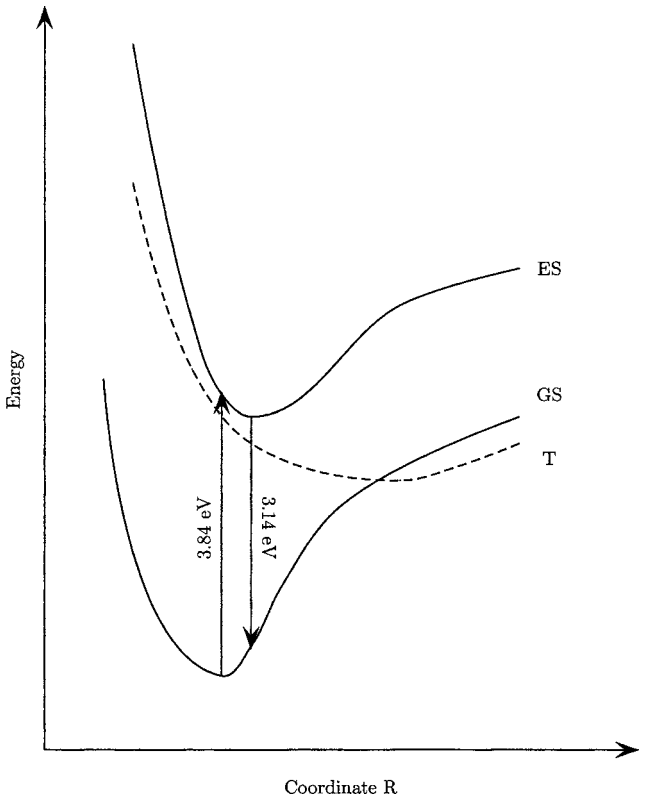

FIG. 4. Schematic potential energy diagram for the ground state (GS), and for the lowest singlet (ES) and triplet excited states (T) of $Si_{29}H_{36}$.

simulate the intensity of the luminescence, whereas the Franck-Condon shifts and the luminescence intensities have been obtained by comparing the excitation energies calculated for the ground state and for the first excited state. Thus, we assume here that the difference between the absorption and emission spectra is only due to the changes in the molecular structure and the corresponding changes in the excitation energies and oscillator strengths.

2. SiH_4, Si_2H_6, and Si_3H_8

The accuracy of the calculated excitation energies were assessed by performing BP and B3LYP TDDFT calculations on SiH_4, Si_2H_6, and Si_3H_8, for which there are accurate experimental data.[44] The calculated and experimental wavelengths are compared in Table I. In the TDDFT calculations, the QZVPP basis sets were used, whereas the molecular structures were optimized using the TZVP basis sets. The excitation wavelengths of the first few strong transitions with oscillator strengths larger than 0.1 are reported. The three first excitation wavelengths obtained in the BP TDDFT calculations using the QZVPP basis sets are 138, 129, and 113 nm (SiH_4); 171, 155, and 148 nm (Si_2H_6); 201, 176, and 167 nm (Si_3H_8). At the B3LYP level, the energies of the first transitions are systematically blueshifted by 4–6 nm as compared to the BP values, whereas the excitation wavelengths of 142, 178, and 205 nm for SiH_4, Si_2H_6, and Si_3H_8 obtained at the SVWN TDDFT level are somewhat larger than the corresponding BP values. The use of the TZVP basis sets in the TDDFT calculation shifts the transitions to higher energies. At the BP DFT level using the TZVP basis sets, the wavelengths of the first transitions are 132, 164, and 195 nm for SiH_4, Si_2H_6, and Si_3H_8, respectively.

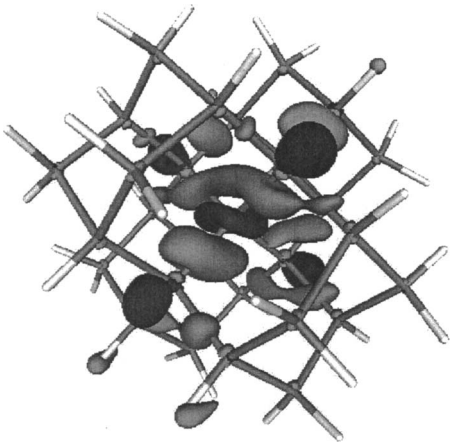

FIG. 5. The change in the charge density upon excitation for $Si_{29}H_{36}$. The electron charge densities of the ground and excited states have been calculated using the ground-state structure of T_d symmetry. Electron accumulation is indicated with dark and depletion with light gray.

For SiH_4, the calculated excitation threshold calculated at the BP DFT level is 0.20 eV larger than the experimental value, whereas for Si_2H_6 and Si_3H_8 they are 0.31 and 0.46 eV too small as compared to the excitation energies deduced from the absorption cross section measurement by Itoh *et al.*[44]

For SiH_4, we obtained at the BP DFT level three strong transitions at 8.96, 9.61, and 10.94 eV which are in good agreement with the experimental values of 8.8, 9.7, and 10.7 eV,[44] whereas in a recent quantum Monte Carlo study by Porter *et al.*[45] only two strong absorption peaks were obtained. At the QMC level, the calculated excitation thresholds for SiH_4 are 9.47(2),[45] 9.1(1),[46] or 9.2,[24] as compared to the present BP TDDFT value of 8.96 eV and the experimental value of 8.8 eV. The QMC approach seems to give systematically a somewhat too large excitation threshold. Porter *et al.*[45] also found that the excitation energies calculated at the LDA level are smaller than the experimental values. However, in the present LDA SVWN calculations we obtained an excitation threshold of 8.8 eV. The obtained results for the small SiH species show that BP TDDFT calculations are able to provide excitation energies in a reasonable agreement with experiment.

3. $Si_{29}H_{36}$

The calculations of the absorption and emission spectra are summarized in Table II. The absorption threshold for the $Si_{29}H_{36}$ cluster calculated at the BP TDDFT level is 3.84 eV and the lowest emission energy is 3.14 eV. The absorption and emission spectra for $Si_{29}H_{36}$ is shown in Fig. 3. In the plot, it was assumed that the transition bands have a Lorentzian band shape with a half-width of 50 meV. For the $Si_{29}H_{36}$ cluster of T_d symmetry, only transitions from excited states of T_2 symmetry contribute to the absorption spectrum.

TABLE III. A comparison of Si—Si bond distances (in pm) for the ground state (GS), the first excited state (ES), and the lowest triplet state (TS) of $Si_{29}H_{36}$ calculated at the BP, PBE, and SVWN DFT levels using the TZVP basis sets. The length of the longest Si—Si bond of the first triplet state is underlined.

Si—Si bond	BP			PBE			SVWN		
	GS	ES	TS	GS	ES	TS	GS	ES	TS
1—2	238.7	239.8	236.3	238.1	239.0	234.9	234.5	235.0	236.8
1—3	238.7	239.8	239.2	238.1	239.0	234.9	234.5	235.0	233.7
1—4	238.7	239.8	237.5	238.1	239.0	234.8	234.5	235.0	253.8
1—26	238.7	239.8	239.0	238.1	239.0	378.3	234.5	235.0	233.1
2—5	238.6	237.6	432.4	238.0	237.1	237.7	234.3	233.5	234.4
2—9	238.6	240.7	236.4	238.0	240.1	238.4	234.3	236.2	234.0
2—10	238.6	240.7	236.0	238.0	240.1	237.6	234.3	236.2	238.2
3—6	238.6	240.7	239.0	238.0	240.1	237.6	234.3	236.2	233.8
3—11	238.6	237.6	238.6	238.0	237.1	237.6	234.3	233.5	234.4
3—12	238.6	240.7	238.9	238.0	240.1	238.4	234.3	236.2	234.5
4—7	238.6	237.6	238.3	238.0	237.1	238.4	234.3	233.5	234.3
4—8	238.6	240.7	238.9	238.0	240.1	237.6	234.3	236.2	237.9
4—13	238.6	240.7	238.7	238.0	240.1	237.6	234.3	236.2	235.1
5—14	237.3	236.6	236.2	237.0	236.4	236.7	233.9	233.3	234.2
5—19	237.3	236.6	235.3	237.0	236.4	237.2	233.9	233.3	233.8
9—15	237.3	237.2	237.1	237.0	236.9	237.2	233.9	234.0	233.4
9—16	237.3	236.9	237.4	237.0	236.6	237.1	233.9	233.6	233.9
11—20	237.3	236.6	237.5	237.0	236.4	236.7	233.9	233.3	234.0
11—25	237.3	236.6	236.6	237.0	236.4	237.1	233.9	233.3	233.9

For the $Si_{29}H_{36}$ cluster in the first singlet excited state, dipole transitions are allowed between the ground state and the excited states belonging to the B_2 and E irreducible representations of the D_{2d} point group. The absorption and the emission spectra of $Si_{29}H_{36}$ have due to the high symmetry of the cluster a rather pronounced peak structure. The intensity of the first transition calculated for the first excited state using its optimized cluster structure is small especially when considering that this transition is experimentally very bright.

Previously, we have shown that the excitation energies calculated at the BP TDDFT level are 0.6–0.7 eV smaller[14,18] than excitation energies obtained at the DFT level using Becke's three-parameter hybrid functional[40] with the Lee-Yang-Parr correlation functional.[41] The excitation threshold for $Si_{29}H_{36}$ calculated at the approximate coupled-cluster singles and doubles[21,22] level was 4.7 eV.[14] The CC2 energy is an upper limit for the excitation energy since the double excitations are considered only implicitly and TZVP is not a very large basis set for coupled-cluster calculations.

The absorption-emission process is schematically shown in Fig. 4. The vertical excitation and deexcitation between the ground and the first excited states are displayed with arrows in the graph. The molecular structure of the excited state undergoes a tiny relaxation giving rise to a Frank-Condon energy shift (ΔE_{FC}) of 0.70 eV. The Si—Si bond lengths and the corresponding changes in the Si—Si distances are given in Table III and the numbering of the atoms for $Si_{29}H_{36}$ is shown in Fig. 1.

The Franck-Condon shift can be divided into two separate contributions; the relaxation of the excited state lowers the excitation energy by 0.30 eV (ΔE_{ES}) and the remaining 0.40 eV is due to the increase of the ground-state energy (ΔE_{GS}) since the cluster structure for the excited state is slightly different from the optimized structure for the ground state.

Franck-Condon shifts calculated at different levels of theory are compared in Table IV and the corresponding energies calculated using the molecular structure optimized for the lowest triplet state are given in Table V. Tables IV and V show that at least GGA functionals and large basis sets must be used in order to obtain reliable structures and energies.

TABLE IV. Comparison of the excitation energies (in eV) and Franck-Condon shifts for $Si_{29}H_{36}$ calculated at DFT levels using TZVP-quality basis sets. The calculated energies are compared to values obtained at the CC2 level using the TZVP basis sets. The oscillator strengths are also given.

	SVWN	BP	PBE	B3LYP	CC2[a]
E_{abs}	3.72	3.84	3.82	4.52	4.68
E_{emi}	3.00	3.14	3.11	3.74	3.84
ΔE_{FC}	0.73	0.70	0.71	0.78	0.84
ΔE_{GS}	0.41	0.40	0.40	0.43	0.45
ΔE_{ES}	0.32	0.30	0.31	0.35	0.39
f_{abs}	0.011	0.012	0.012	0.018	0.015
f_{emi}	0.0010	0.0017	0.0014	0.0019	0.0031

[a]Single-point calculations for geometries optimized at the BP DFT level using the TZVP basis sets.

TABLE V. Comparison of the excitation energies (in eV) and Franck-Condon shifts for $Si_{29}H_{36}$ calculated at DFT levels using TZVP-quality basis sets. The energies have been obtained using the optimized molecular structures for the lowest triplet state. The oscillator strengths are also given.

	SVWN	BP	PBE	B3LYP
E_{abs}	3.72	3.84	3.82	4.52
E_{emi}	1.83	1.21	1.84	1.84
ΔE_{FC}	1.89	2.64	1.98	2.68
ΔE_{GS}	1.38	1.44	1.06	1.01
ΔE_{ES}	0.51	1.20	0.92	1.67
f_{emi}	0.0031	0.104	0.103	0.143

For the ground-state structure, the lowest triplet state lies 0.12 eV below the first excited singlet state, but the optimization of the molecular structure of the triplet states lowers its energy such that it even becomes lower in energy than the lowest singlet state. This state crossing results in convergence problems in the TDDFT optimization of the triplet state. The optimization of the triplet state at the unrestricted DFT level yields a totally nonsymmetric (C_1) structure for the $Si_{29}H_{36}$ cluster. For the optimized structure of the triplet state, the triplet state becomes the ground state of the $Si_{29}H_{36}$ cluster showing that one should be careful with the use of the optimized triplet-state structure as a substitute for the optimized structure of the first excited singlet state. The optimized molecular structures of the lowest triplet state and that of the first excited singlet state are in this case completely different. This also means that conclusions drawn from calculations on the lowest triplet state might be misleading. Franceschetti and Pantelides[13] obtained very large Frank-Condon shifts of 2.92 eV for $Si_{29}H_{36}$ by using the lowest triplet state to estimate the molecular structure of the first excited singlet state. The present study suggests that such a large Frank-Condon shift is an artifact of the computational method used. The present Frank-Condon shift of 0.7 eV calculated at the BP TDDFT level is also in better agreement with experimental observations.

The charge-density difference between the ground state and the first excited singlet state of $Si_{29}H_{36}$ has been calculated at the BP DFT level using first-order linear-response theory. The density difference shows that the exciton, or the electron-hole pair, is mainly located close to the interior part of the Si cluster. As seen in Figs. 5 and 6, the difference in the exciton densities calculated using the ground-state and the excited-state structures is small. A density threshold of 0.001 e Å^{-3} was used in the plots. The excited state has a small surplus of electrons in the vicinity of the central Si atom, whereas further away from it the ground state has an excess of electrons as compared to the excited state. For both structures, the exciton density is smeared out over the entire cluster.

4. $Si_{29}H_{24}$ and $Si_{35}H_{36}$

For $Si_{29}H_{24}$, the Franck-Condon shift obtained at the BP TDDFT level is 1.17 eV which can be divided into a ΔE_{GS} of 0.48 eV and a ΔE_{ES} contribution of 0.44 eV. For $Si_{35}H_{36}$, the corresponding energies are 1.67 (ΔE_{FC}), 1.19 (ΔE_{GS}), and 0.48 eV (ΔE_{ES}). The Frank-Condon shifts of the studied Si nanoclusters are compared in Table II. The absorption thresholds for $Si_{29}H_{24}$ and $Si_{35}H_{36}$ are 2.74 and 3.70 eV, respectively. However, the large Franck-Condon shifts of 1.17 and 1.67 eV indicate that these clusters do not emit blue light as observed experimentally but they should instead emit light at 610 and 790 nm, respectively. Thus, the calculated luminescence energies of 1.57 and 2.03 eV show that it is most unlikely that these clusters are the one obtained in the etching process.

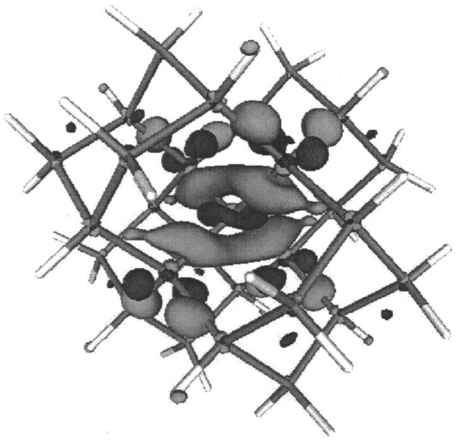

FIG. 6. The change in the charge density up on excitation for $Si_{29}H_{36}$. The electron charge densities of the ground and excited states have been calculated using the excited-state structure of D_{2d} symmetry. Electron accumulation is indicated with dark and depletion with light gray.

The calculated absorption and emission spectra for $Si_{29}H_{24}$ and $Si_{35}H_{36}$ are shown in Figs. 7 and 8, respectively. In the plots, we assumed Lorentzian band shapes with a half-width of 50 meV. Since the ground-state structure of $Si_{29}H_{24}$ and $Si_{35}H_{36}$ are of T_d symmetry, transitions from T_2 excited states contribute to the absorption spectrum. For the excited-state structure of $Si_{29}H_{24}$ possessing C_s symmetry, all transitions are dipole allowed. The same is true for the nonsymmetric (C_1) structure of the excited state of the $Si_{35}H_{36}$ cluster. Since all transitions are dipole allowed, the intensity of the emission spectra is smeared out over a large energy

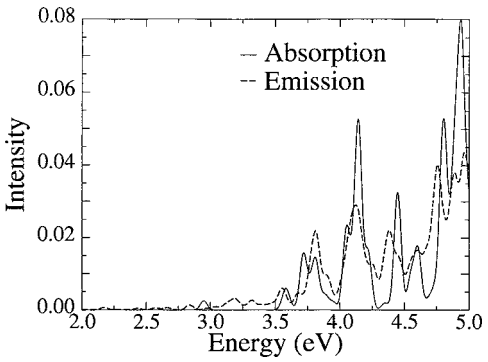

FIG. 7. The absorption and emission spectra of the $Si_{29}H_{24}$ cluster calculated at the BP DFT level using the TZVP basis sets.

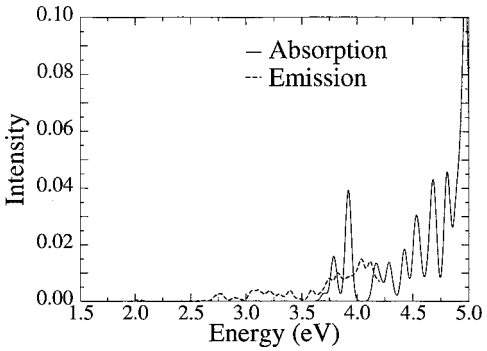

FIG. 8. The absorption and emission spectra of the $Si_{35}H_{36}$ cluster calculated at the BP DFT level using the TZVP basis sets.

interval yielding a flat curve without distinguished transition peaks. The band strengths of the emission spectra are very weak as compared to the strong luminescence observed experimentally.

IV. CONCLUSIONS

The electronic excitation spectra of the $Si_{29}H_{24}$, $Si_{29}H_{36}$, and $Si_{35}H_{36}$ nanoclusters have been studied using density-functional theory. The calculations show that for $Si_{29}H_{36}$ and $Si_{35}H_{36}$ absorption threshold lies in the ultraviolet region (320–340 nm), whereas for $Si_{29}H_{24}$ it is at about 450 nm. The Si nanoclusters were found to have large Franck-Condon shifts of 1.17, 0.70, and 1.67 eV for $Si_{29}H_{24}$, $Si_{29}H_{36}$, and $Si_{35}H_{36}$, respectively. The calculated deexcitation energies of 1.57, 3.14, and 2.03 eV for the three Si clusters correspond to luminescence wavelengths of 790, 395, and 620 nm. In the experimental emission spectrum, the strong luminescence band appears at 400 nm,[17] suggesting that it is most likely that of these candidates it is the luminescence from the $Si_{29}H_{36}$ cluster that is observed. The oscillator strength for the deexcitation from the first excited singlet state to the ground state is significantly smaller than what one would expect for a strongly luminescent species. The calculations suggest that there are other factors than dipole transition moments that determine the luminescence strength of the silicon clusters.

For $Si_{29}H_{24}$ and $Si_{29}H_{36}$, the Franck-Condon shifts were found to be almost equally divided between contributions from the relaxation of the excited state and from the strain of the ground state, whereas for the Franck-Condon shift of $Si_{35}H_{36}$, the strain of the ground state contributes more than twice the relaxation energy of the excited state.

The structure optimization of the triplet state shows that the molecular structure of the triplet state and the molecular structure of the first excited state are completely different. Thus, the molecular structure for the triplet state of the $Si_{29}H_{36}$ cluster calculated at the unrestricted DFT level is not a good substitute for the optimized structure of the first excited singlet state, as recently proposed by Franceschetti and Pantelides.[13] The unrestricted DFT optimization and the TD-DFT optimization of the triplet state using the GGA functionals yield molecular structures with a dissociated Si—Si bond, whereas the TDDFT optimization of the molecular structure of the first singlet state involves only small changes in the structure.

The present study also shows that density functionals of at least GGA type should be employed in DFT studies of silicon clusters, since DFT calculations at the LDA level seem occasionally to provide misleading cluster structures.

ACKNOWLEDGMENTS

We acknowledge financial support from the European research training network on "Understanding Nanomaterials from a Quantum Perspective" (NANOQUANT), Contract No. MRTN-CT-2003-506842, from the Nordisk Forskerakademi network for research and research training (NorFA Grant No. 030262) on "Quantum Modeling of Molecular Materials" (QMMM), from The Academy of Finland (FA Projects No. 53915, No. 200903, and No. 206102), from Magnus Ehrnrooth's Foundation, and from "Tekniska Vetenskapsakademien i Finland." We also thank Professor Reinhart Ahlrichs (Karlsruhe) for an up-to-date version of the TURBOMOLE program package.

[1] L. T. Canham, Appl. Phys. Lett. **57**, 1046 (1990).
[2] C. Pickering, L. T. Canham, and D. Brumhead, Appl. Surf. Sci. **63**, 22 (1993).
[3] A. G. Cullis, L. T. Canham, and J. P. Calcott, J. Appl. Phys. **82**, 909 (1997).
[4] M. H. Nayfeh, O. Akcakir, J. Terrien, Z. Yamani, N. Barry, W. Yu, and E. Gratton, Appl. Phys. Lett. **75**, 4112 (1999).
[5] O. Akcakir, J. Terrien, G. Belomoin, N. Barry, J. D. Muller, E. Gratton, and M. H. Nayfeh, Appl. Phys. Lett. **76**, 1857 (2000).
[6] G. Belomoin, J. Terrien, and M. H. Nayfeh, Appl. Phys. Lett. **77**, 779 (2000).
[7] M. H. Nayfeh, N. Barry, J. Terrien, O. Akcakir, E. Gratton, and G. Belomoin, Appl. Phys. Lett. **78**, 1131 (2001).
[8] G. Belomoin, J. Terrien, A. Smith, S. Rao, R. Twesten, S. Chaieb, L. Wagner, L. Mitas, and M. H. Nayfeh, Appl. Phys. Lett. **80**, 841 (2002).
[9] M. H. Nayfeh, in *Atoms, Molecules and Quantum Dots in Laser Fields: Fundamental Processes*, edited by N. Bloembergen, N. Rahman, and A. Rizzo, Conference Proceedings Vol. 71 (Società Italiana di Fisica, Bologna, 2001), pp. 83–96.
[10] M. H. Nayfeh, S. Rao, N. Barry, J. Therrien, G. Belomoin, A. Smith, and S. Chaieb, Appl. Phys. Lett. **80**, 121 (2002).
[11] M. H. Nayfeh, O. Akcakir, G. Belomoin, N. Barry, J. Therrien, and E. Gratton, Appl. Phys. Lett. **77**, 4086 (2000).
[12] L. Mitas, J. Terrien, R. Twesten, G. Belomoin, and M. H. Nayfeh, Appl. Phys. Lett. **78**, 1918 (2001).
[13] A. Franceschetti and S. T. Pantelides, Phys. Rev. B **68**, 033313 (2003).

[14] D. Sundholm, Nano Lett. **3**, 847 (2003).
[15] Z. Zhou, L. Brus, and R. A. Friesner, J. Am. Chem. Soc. **125**, 15599 (2003).
[16] Z. Zhou, R. A. Friesner, and L. Brus, Nano Lett. **3**, 163 (2003).
[17] S. Rao, J. Sutini, R. Clegg, E. Gratton, M. H. Nayfeh, S. Habbal, A. Tsolakidis, and R. M. Martin, Phys. Rev. B **69**, 205319 (2004).
[18] D. Sundholm, Phys. Chem. Chem. Phys. **6**, 2044 (2004).
[19] E. W. Draeger, J. C. Grossman, A. Williamson, and G. Galli, Phys. Rev. Lett. **90**, 167402 (2003).
[20] G. Belomoin, E. Rogozhina, J. Terrien, P. V. Braun, L. Abuhassan, M. H. Nayfeh, L. Wagner, and L. Mitas, Phys. Rev. B **65**, 193406 (2002).
[21] O. Christiansen, H. Koch, and P. Jørgensen, Chem. Phys. Lett. **243**, 4041 (1995).
[22] C. Hättig and F. Weigend, J. Chem. Phys. **113**, 5154 (2000).
[23] A. Puzder, A. J. Williamson, J. C. Grossman, and G. Galli, J. Am. Chem. Soc. **125**, 2786 (2003).
[24] L. X. Benedict, A. Puzder, A. J. Williamson, J. C. Grossman, G. Galli, J. E. Klepeis, J. Y. Raty, and O. Pankratov, Phys. Rev. B **68**, 085310 (2003).
[25] C. S. Garoufalis, A. D. Zdetsis, and S. Grimme, Phys. Rev. Lett. **87**, 276402 (2001).
[26] A. Williamson, J. C. Grossman, R. Q. Hood, A. Puzder, and G. Galli, Phys. Rev. Lett. **89**, 196803 (2002).
[27] S. H. Vosko, L. Wilk, and M. Nusair, Can. J. Phys. **58**, 1200 (1980).
[28] J. P. Perdew, Phys. Rev. B **33**, 8822 (1986).
[29] A. D. Becke, Phys. Rev. A **38**, 3098 (1988).
[30] A. Schäfer, C. Huber, and R. Ahlrichs, J. Chem. Phys. **100**, 5829 (1994).
[31] R. Bauernschmitt and R. Ahlrichs, Chem. Phys. Lett. **256**, 454 (1996).
[32] R. Bauernschmitt, M. Häser, O. Treutler, and R. Ahlrichs, Chem. Phys. Lett. **264**, 573 (1997).
[33] F. Furche, J. Chem. Phys. **114**, 5982 (2001).
[34] F. Furche and R. Ahlrichs, J. Chem. Phys. **117**, 7433 (2002).
[35] P. A. M. Dirac, Proc. Cambridge Philos. Soc. **26**, 376 (1930).
[36] J. C. Slater, Phys. Rev. **81**, 385 (1951).
[37] K. Eichkorn, O. Treutler, H. Öhm, M. Häser, and R. Ahlrichs, Chem. Phys. Lett. **240**, 283 (1995).
[38] J. P. Perdew, K. Burke, and M. Ernzerhof, Phys. Rev. Lett. **77**, 3865 (1996).
[39] J. Tao, J. P. Perdew, V. N. Staroverov, and G. E. Scuseria, Phys. Rev. Lett. **91**, 146401 (2003).
[40] A. D. Becke, J. Chem. Phys. **98**, 5648 (1993).
[41] C. Lee, W. Yang, and R. G. Parr, Phys. Rev. B **37**, 785 (1988).
[42] R. Ahlrichs, M. Bär, M. Häser, H. Horn, and C. Kölmel, Chem. Phys. Lett. **162**, 165 (1989); current version available at http://www.turbomole.de
[43] F. Jensen, *Introduction to Computational Chemistry* (Wiley, Chichester, 1999).
[44] U. Itoh, Y. Yasutake, H. Onuki, N. Washida, and T. Ibuki, J. Chem. Phys. **85**, 4867 (1986).
[45] A. R. Porter, M. D. Towler, and R. J. Needs, Phys. Rev. B **64**, 035320 (2001).
[46] J. C. Grossman, M. Rohlfing, L. Mitas, S. G. Louie, and M. L. Cohen, Phys. Rev. Lett. **86**, 472 (2001).